

Shape-Dependent Confinement in Ultrasmall Zero-, One-, and Two-Dimensional PbS Nanostructures

Somobrata Acharya,^{*,†,‡} D. D. Sarma,^{‡,§} Yuval Golan,^{||} Sucheta Sengupta,[‡] and Katsuhiko Ariga[†]

World Premier International (WPI) Research Center for Materials Nanoarchitectonics (MANA), National Institute for Materials Science (NIMS), 1-1 Namiki, Tsukuba, Ibaraki 305-0044, Japan, Centre for Advanced Materials, Indian Association for the Cultivation of Science, Kolkata 700032, India, Solid State and Structural Chemistry Unit and Centre for Condensed Matter Theory, Indian Institute of Science, Bangalore 560012, India, and Department of Materials Engineering and the Ilse Katz Institute for Meso and Nanoscale Science and Technology, Ben-Gurion University of the Negev, Beer-Sheva 84105, Israel

Received May 1, 2009; E-mail: camsa2@iacs.res.in

Spatial dimensionality affects the degree of confinement when an electron–hole pair is squeezed from one or more dimensions approaching the bulk exciton Bohr radius (a_B) limit.¹ In zero-dimensional (0D) dots, the charge carriers are confined in all three dimensions (3D-confined); in one-dimensional (1D) wires/rods, the charges are confined in two spatial directions (2D-confined), whereas in two-dimensional (2D) sheets, the restricted thickness is the sole confinement dimension (the charges are 1D-confined). Thus, the geometry influences the spatial confinement of the carriers, which can lead to a variety of novel perspectives for fundamental science as well as potentially useful device applications. Theoretical studies have revealed an enhancement of the electron–hole interaction depending on confined dimensions in the order 0D > 1D > 2D.² However, experimental reports on dimensionality-controlled nanostructures dealing with all three shapes (0D, 1D, and 2D) retaining at least one comparable dimension in the very strong confinement regime have been rare, and this remains a key obstacle in characterizing novel nanoscale properties in the very strong confinement regime.³ Thus, a large number of opportunities could be realized by producing dimensionality-controlled nanostructures in the very strong confinement regime, which could lead to the success of potential applications. Here we report the controlled synthesis of PbS nanomaterials with 0D, 1D, and 2D forms retaining at least one dimension in the strongly confined regime far below a_B (~20 nm for PbS) and provide evidence through varying the exciton–phonon coupling strength that the degree of confinement is systematically weakened by the loss of confinement dimension. Geometry variations reflect distinguishable far-field optical polarizations, which could find useful applications in polarization-sensitive devices.

The synthesis of dimensionality-controlled nanostructures was carried out using trioctylamine (TOA) as a liganding solvent that enables low-temperature decomposition of the single precursor lead ethyl or hexadecyl xanthate [see the Supporting Information (SI)].⁴ Transmission electron microscopy (TEM; Figure 1) shows the 0D spherical dots with an average diameter of 6 nm and a distribution of 10–13% synthesized using 3 mL of TOA at 65 °C (see the SI). Control over the anisotropy was imposed by lead hexadecyl xanthate and annealing at elevated temperature (80 °C) to obtain free-standing rods of 12–15 nm in length and 1.7 nm in width (see the SI).^{4b} Ultrathin strictly 2D sheets with dimensions of 40–50 nm in length and ~25 nm in width were obtained by injecting lead

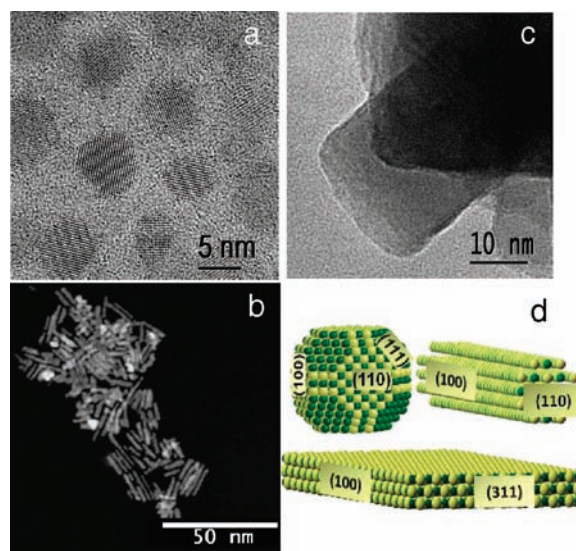


Figure 1. Bright- and dark-field TEM images of ultranarrow PbS (a) dots, (b) rods, and (c) sheets. (d) Reconstructed images of the sphere, rod, and sheet constructed using unit cells with lead (green) and sulfur (yellow) ions matching the closest dimensions of the materials.

ethyl xanthate at 60 °C and annealing the reaction at an elevated temperature of 100 °C for 80 min (see the SI). High-resolution TEM (HRTEM) and selected-area electron diffraction (SAED) revealed that the dots, rods, and sheets are single-crystalline with the PbS rock-salt structure (see the SI). Energy-dispersive spectroscopy (EDS) analysis carried out in the TEM (see the SI) showed a Pb/S stoichiometric ratio of ~1:1 for the dots, rods, and sheets (see the SI).

The coupling of electronic states to the optical phonons is accompanied by a coupling strength that depends on the spatial extent of the exciton, and hence, coupled mode frequencies depend on the particle shape and size.⁵ The dependence of the degree of quantum confinement on confined geometry is indeed reflected in the Raman spectra recorded with different excitation wavelengths (Figure 2a,b). All of the geometrically confined nanoshapes show multiphonon structures at energies that are nearly multiples of the first-order peaks with multiple excitation wavelengths. Notably, the peaks for 0D dots are considerably broadened and shifted to higher wavenumber relative to those for the other shapes, and the peak positions follow a shift in the order sheet < rods < dots, reflecting the increasing dimensionality of confinement. The strength of the exciton–phonon coupling strongly increases for the phonons whose wavelength matches with the spatial extent of the exciton; the

[†] National Institute for Materials Science.

[‡] Indian Association for the Cultivation of Science.

[§] Indian Institute of Science.

^{||} Ben-Gurion University of the Negev.

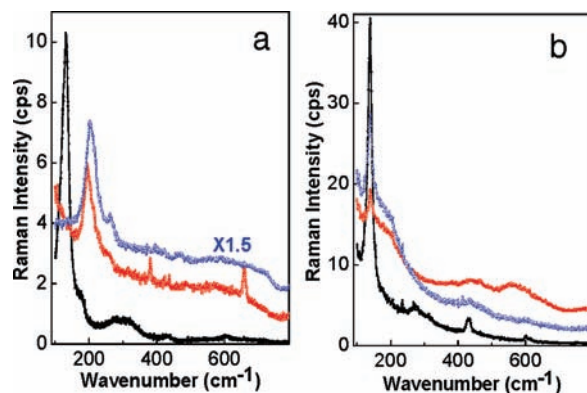


Figure 2. Uncorrected confocal Raman spectra for cast films of 0D dots (blue curves), 1D rods (red curves), and 2D sheets (black curves) at 300 K with excitation at (a) 644 nm using a He–Ne laser line (the dot spectrum has been multiplied by a factor 1.5 for clarity) and (b) 514 nm using an Ar⁺ laser line.

Fröhlich interaction should decrease rapidly with the increase in the degree of confinement.⁵ In the adiabatic approximation, the efficiency of Fröhlich coupling is characterized by the dimensionless Huang–Rhy parameter, which can be determined from the intensity ratio as $S_{K(\text{exptl})} = KI_K/I_{K-1}$, where I_K is the intensity of the K -phonon satellite.^{5,6} The ratio of the first overtone (2LO) mode intensity to the fundamental (1LO) mode intensity, $I_{2\text{LO}}/I_{1\text{LO}}$, which reflects the exciton–phonon coupling strength, decreases with increasing degree of confinement at both excitation wavelengths (see the SI). The ratio varied from 0.49 for the sheets down to 0.10 for the dots with 644 nm excitation and from 0.70 to 0.34 with 514 nm excitation. A relatively smaller difference in the ratio was observed between the rods and the dots, reflecting the degree of confinement.

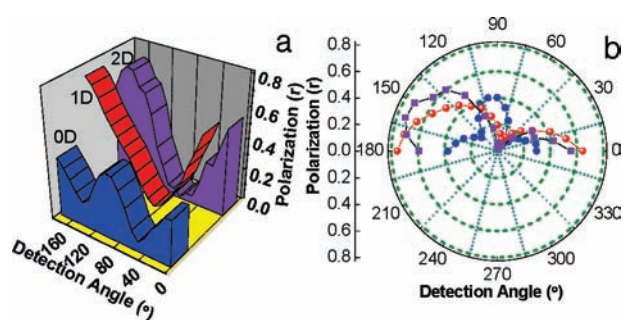


Figure 3. (a) Polarization-angle-resolved photoluminescence spectra of organized monolayer LB films lifted onto glass slides for 0D dots (blue filled curve), 1D rods (red ribbon curve), and 2D sheets (violet filled curve) with emission monitored at 410 nm. (b) Polar plot of the polarization dependence for 0D dots (blue dots), 1D rods (red squares), and 2D sheets (violet squares).

A beneficial way of examining the effect of dimensionality is to explore the optical polarization of dimensionality-controlled nanostructures.^{4a,7} Optimal packing of the materials was achieved using the Langmuir–Blodgett (LB) technique to gain insight into the role of geometry on the optical polarization, taking advantage of the in-plane orientation of the nanostructures.^{4a,7} The polarization was determined by fitting the intensity ratio $r = (I_{\parallel} - I_{\perp})/I_{\parallel}$ versus detection angle with a sine-squared function, where I_{\parallel} (I_{\perp}) is the intensity parallel (perpendicular) to the long $\langle 110 \rangle$ axis of the rods (Figure 3a,b). For the rods, the polarization r was found to be 0.85

± 0.05 , showing their high degree of anisotropy. Notably, the 0D dots reveal a much smaller degree of polarization, and the direction of polarization sinusoidally oscillates, showing a dip at each $\sim 45^\circ$ angle of detection. The planar degenerate transition dipoles and “dark axis” in a plane normal to the transition dipoles possibly exists in such symmetric dots.^{2b,c} The assignment of a specific polarization direction for a closed packed layer of 2D sheets is rather difficult because of its 2D geometry. However, the 2D sheets may be treated as a biaxial crystal with $\langle 100 \rangle$ and $\langle 113 \rangle$ in-plane directions. Individual polarization along these crystallographic directions should show a dependence at an angle of 72° apart, which is close to our result of 65° (Figure 3). Simultaneous contributions from these axes result in in-plane optical anisotropies, the extent of which is maximized from the contribution of the long axis, considering that the rectangular nature might have caused the observed shift in polarization. In fact, the strongest degree of polarization dependence is expected for the 1D rods among these nanostructures because of a definite polarization vector oriented parallel to the quantization axis, as reflected in Figure 3. The compressed layer can be transferred onto a variety of planar substrates (glass, quartz, gold, etc.) as mono- or multilayers of alternative shapes by LB deposition with a transfer ratio close to unity per monolayer. This process of planar nanoscale assembly is advantageous for the fabrication of complex network patterns with combinations of differently shaped particles. In summary, we have shown the impact of dimension on quantum confinement by designing PbS nanomaterials into ultrasmall quantum dots (0D), quantum rods (1D), and quantum sheets (2D) in the strong confinement regime. These shape-controlled structures exhibit electron–phonon interactions along with robust geometry-driven optical polarization dependence. Large surface coverage of these materials in highly oriented LB films is advantageous for orientation-sensitive optoelectronic devices.

Acknowledgment. Financial support from the Centre for Nanotechnology for Photovoltaics and Sensor Devices, DST, Government of India (Grant SR/S5/NM-47/2005) and the World Premier International Research Center (WPI) Initiative on Materials Nanoarchitectonics, MEXT, Japan, are gratefully acknowledged.

Supporting Information Available: HRTEM, SAED, and EDS data; a table of multiple LO frequencies; and surface pressure–area isotherms. This material is available free of charge via the Internet at <http://pubs.acs.org>.

References

- (1) (a) Nozik, J. *Annu. Rev. Phys. Chem.* **2001**, *52*, 193. (b) Yoffe, Y. D. *Adv. Phys.* **1993**, *42*, 173. (c) Mokari, T.; Zhang, M.; Yang, P. *J. Am. Chem. Soc.* **2007**, *129*, 9864.
- (2) (a) D’Andrea, A.; Del Sole, R. *Phys. Rev. B* **1990**, *41*, 1413. (b) Empedocles, S. A.; Neuhäuser, R.; Bawendi, M. G. *Nature* **1999**, *399*, 126. (c) Efros, A. L.; Rosen, M.; Kuno, M.; Nirmal, M.; Norris, D. J.; Bawendi, M. *Phys. Rev. B* **1996**, *54*, 4843.
- (3) (a) Yu, H.; Li, J.; Loomis, R. A.; Wang, L.; Buhro, W. E. *Nat. Mater.* **2003**, *2*, 517. (b) Zhu, Q.; Karlsson, K. F.; Pelucchi, E.; Kapon, E. *Nano Lett.* **2007**, *7*, 2227. (c) Yu, H.; Li, J.; Loomis, R. A.; Gibbons, P. C.; Wang, L.; Buhro, W. E. *J. Am. Chem. Soc.* **2003**, *125*, 16168. (d) Buhro, W.; Colvin, V. L. *Nat. Mater.* **2003**, *2*, 138.
- (4) (a) Patla, I.; Acharya, S.; Zeiri, L.; Israelachvili, J.; Efrima, S.; Golan, Y. *Nano Lett.* **2007**, *7*, 1459. (b) Acharya, S.; Gautam, U. K.; Sasaki, T.; Bando, Y.; Golan, Y.; Ariga, K. *J. Am. Chem. Soc.* **2008**, *130*, 4594.
- (5) Alivisatos, A. P.; Harris, T. D.; Carroll, P. J.; Steigerwald, M. L.; Brus, L. E. *J. Chem. Phys.* **1989**, *90*, 3463.
- (6) (a) Schmitt-Rink, S.; Miller, D. A. B.; Chemla, D. S. *Phys. Rev. B* **1987**, *35*, 8113. (b) Devreese, J. T.; Fomin, V. M.; Gladilin, V. N.; Pokatilov, E. P.; Klimin, S. N. *Nanotechnology* **2002**, *13*, 163.
- (7) (a) Acharya, S.; Patla, I.; Kost, J.; Efrima, S.; Golan, Y. *Adv. Mater.* **2007**, *19*, 1105. (b) Acharya, S.; Patla, I.; Kost, J.; Efrima, S.; Golan, Y. *J. Am. Chem. Soc.* **2006**, *128*, 9294.

JA903539D